MURDOCH RESEARCH REPOSITORY

*This is the author's final version of the work, as accepted for publication following peer review but without the publisher's layout or pagination.
The definitive version is available at*
http://dx.doi.org/10.1139/cjfas-2015-0422

Hordyk, A.R., Ono, K., Prince, J.D. and Walters, C.J. (2016) A simple length-structured model based on life history ratios and incorporating size-dependent selectivity: application to spawning potential ratios for data-poor stocks. Canadian Journal of Fisheries and Aquatic Sciences, 73 (12). pp. 1787-1799.

http://researchrepository.murdoch.edu.au/34644/

Canadian Journal of Fisheries and Aquatic Sciences
Journal canadien des sciences halieutiques et aquatiques

A simple length-structured model based on life history ratios and incorporating size-dependent selectivity: application to spawning potential ratios for data-poor stocks

SCHOLARONE™
Manuscripts

Title Page

A simple length-structured model based on life history ratios and incorporating size-dependent selectivity: application to spawning potential ratios for data-poor stocks

Authors:

Adrian R. Hordyk[1*], Kotaro Ono[2], Jeremy D. Prince[1,3], and Carl J. Walters[4]

Author affiliations:

* Corresponding author, tel: +61 893606685; fax: +618 9360 6303; e-mail: a.hordyk@murdoch.edu.au

1. Centre for Fish and Fisheries Research, Murdoch University, 90 South Street, Murdoch, Western Australia 6150, Australia

2. School of Aquatic and Fishery Sciences
   Box 355020, University of Washington, Seattle, WA 98195-5020, U.S.A., kotarono@uw.edu

3. Biospherics Pty Ltd, PO Box 168, South Fremantle, WA 6162, Australia, biospherics@ozemail.com.au

4. Fisheries Centre, University of British Columbia, Vancouver B.C. V6T1Z4, Canada, c.walters@fisheries.ubc.ca

1

1   **Abstract**

2   Selectivity in fish is often size-dependent, which results in differential fishing

3   mortality rates across fish of the same age; an effect known as "Lee's Phenomenon". We

4   extend previous work on using length composition to estimate the spawning potential ratio

5   (SPR) for data-limited stocks by developing a computationally efficient length-structured per-

6   recruit model that splits the population into a number of sub-cohorts, or growth-type-groups,

7   to account for size-dependent fishing mortality rates. Two simple recursive equations, using

8   the life-history ratio of the natural mortality rate to the von Bertalanffy growth parameter

9   (M/K), were developed to generate length composition data, reducing the complexity of the

10 previous approach. Using simulated and empirical data we demonstrate that ignoring Lee's

11 Phenomenon results in over-estimates of fishing mortality and negatively biased estimates of

12 SPR. We also explored the behaviour of the model under various scenarios, including

13 alternative life-history strategies, and the presence of size-dependent natural mortality. The

14 model developed in this paper may be a useful tool to estimate the spawning potential ratio

15 for data-limited stock where it is not possible to apply more conventional methods.

16

17 **Key words**: stock assessment; data-poor; simulation; growth-type-groups

18

2

Introduction

19

20   In order to maintain the long-term stability of yield from capture fisheries, the

21 dynamics of fish populations and the impact of harvesting these populations must be

22 understood. While there have been some notable failures, the quantitative methods of

23 fisheries science are generally accepted as reliable and useful tools for managing fisheries

24 (Hilborn 2007, Hilborn and Ovando 2014). However, many conventional methods require

25 large amounts of data, including reliable biological information on the exploited stock and a

26 historical time series of total removals (Kelly et al. 2006, Bentley 2015). Many fisheries,

27 particularly in (but certainly not restricted to) developing regions, do not have the data

28 required for conventional methods and are considered data-limited or data-poor (Bentley

29 2015, Costello et al. 2015). The severity of the problem is further exemplified by the fact that

30 many of the world's data-poor stocks are in areas of high marine biodiversity, high

31 population density, low management capacity, and considerable poverty (Andrew et al. 2007,

32 Worm and Branch 2012, Pitcher and Cheung 2013). Furthermore, the inhabitants of these

33 nations are often disproportionally reliant on fish as vital sources of protein, and fisheries

34 play an important role providing livelihoods for millions of people (Kent 1997, Béné 2003,

35 Walmsley et al. 2006). The immensity of the problem faced by managers of data-poor

36 fisheries is recognised by the fisheries science community, and an increasing literature on the

37 development of alternative methods for data-poor fisheries has been building in recent years

38 (e.g., Honey et al. 2010, Dowling et al. 2015, Kokkalis et al. 2015, Jardim et al. 2015, Hordyk

39 et al. 2015a, Thorson and Cope 2015, Prince et al. 2015a, Roa-Ureta et al. 2015, Roa-Ureta

40 2015, Needle 2015).

41   The length-based spawning potential ratio (LB-SPR) method is an example of an

42 assessment method that was recently developed as a tool for assessing and managing data-

43 poor fisheries (Hordyk et al. 2015b, 2015b, Prince et al. 2015b). The LB-SPR method uses

44 estimates of the life history ratio of natural mortality (M) to the K parameter from the von

45 Bertalanffy growth equation (M/K) to estimate the spawning potential ratio (SPR) from size

46 composition data of an exploited stock. The M/K ratio is known to vary less within stocks of

47 the same species, or closely related species, than the individual M and K parameters

48 (Beverton 1992), and can be estimated from meta-analysis or comparative studies (Prince et

49 al. 2015a, 2015b). By using the life-history ratio $M/K,$ the LB-SPR model avoids the reliance

50 on the natural mortality parameter, which, especially for exploited stocks, is notoriously

51 difficult to estimate (Kenchington 2014). Furthermore, the length frequency of the catch is

3

52 one of the cheapest and easiest forms of data to collect (Quinn and Deriso 1999), although

53 careful and well-structured sampling is required to ensure that the data are representative

54 (Erzini 1990, Gerritsen and McGrath 2006, Heery and Berkson 2009).

55   Hordyk et al. (2015b) demonstrated that, with the assumption of a knife-edge

56 selectivity pattern, the expected size frequency of the catch and the spawning potential ratio

57 of the stock could be represented by simple analytical models using the ratios M/K, relative

58 fishing mortality to natural mortality (F/M), and the relative size at first capture to the

59 asymptotic length (L_c/L_∞), without requiring estimates of the individual parameters M, F or K.

60 Incorporating non-knife-edge selectivity patterns was more complex, and an age-structured

61 model parametrized in terms of the life history ratios was required (Hordyk et al. 2015b,

62 2015c). In this paper we develop a per-recruit length-structured model which can account for

63 a range of selectivity patterns and can be represented by two simple recursive equations.

64   It is often assumed in fisheries assessment models that length-at-age is normally

65 distributed, with the mean length-at-age described by the von Bertalanffy growth equation.

66 Selectivity is often, although not always, observed to be size-related rather than dependent on

67 age (Francis 2015), and faster growing fish are expected to reach the length at which they are

68 vulnerable to the fishing gear before the slower growing individuals, and thus are exposed to

69 a higher cumulative fishing mortality throughout their lifetime. As a result, when subject to

70 fishing mortality, the size-at-age distribution of older age classes is no longer normally

71 distributed, as the larger individuals in each age class are reduced in number relative to the

72 smaller individuals in the same age class. This effect, first documented over 100 years ago

73 (Lee 1912), has since become referred to as "Lee's Phenomenon". Although the effect is

74 often ignored in age-structured models, a number of techniques have been developed to

75 account for Lee's Phenomenon in fisheries assessments by dividing the modelled fish

76 population into a number of sub-populations and tracking the sub-cohorts over time (Punt et

77 al. 2002, Walters and Martell 2004, McGarvey et al. 2007, Taylor and Methot 2013). The

78 age-structured LB-SPR model did not account for Lee's Phenomenon, and is therefore

79 expected to over-estimate fishing mortality when selectivity is size-dependent. In this paper,

80 we extend the new length-structured model using the growth-type-group (GTG) approach of

81 Walters and Martell (2004) to account for Lee's Phenomenon. This new per-recruit model

82 (referred to as the GTG LB-SPR model) uses the life history ratio M/K, together with

83 estimates of size-at-maturity and asymptotic size (L_∞) and length composition data, to

84 estimate the spawning potential ratio of data-limited stocks with size-dependent selectivity

85 patterns.

4

86   We first used a simulation model to explore the effect of the different parameters of

87   the GTG LB-SPR model on the predicted equilibrium size composition and the resulting

88   level of SPR. We then compared the estimates of the newly developed GTG LB-SPR model,

89   and the original LB-SPR model (Hordyk et al. 2015b, 2015c), by applying the two methods

90   to both simulated and empirical data sets. Similar to the LB-SPR model, the GTG LB-SPR

91   model developed here assumes known life history parameters, and uses an equilibrium per-

92   recruit model to estimate the relative fishing mortality, selectivity-at-length, and the

93   spawning potential ratio, from representative catch-at-length data.

94

95   **Methods**

96   **Derivation of Length-Structured Per-Recruit Model to Predict Size Composition**

97   *Per-recruit number at length*

98   Fish growth is typically described by the von Bertalanffy growth equation, which is

99   commonly written as:

$$L(a) = L_\infty\left(1 - e^{-K(a-t_0)}\right) \tag{1}$$

100   where $L(a)$ is the length at age a, L_∞ is the mean asymptotic length, K is the von Bertalanffy

101   growth parameter, and t_0 is the hypothetical, usually negative, age at which length is zero.

102   The von Bertalanffy growth model can be reparametrized by replacing t_0 with a more

103   biologically meaningful parameter L_0, the initial length at age 0:

$$L(a) = L_\infty\left(1 - \left(1 - \frac{L_0}{L_\infty}\right)e^{-Ka}\right) \tag{2}$$

104   Assuming for simplicity that L_0 is zero gives:

$$L(a) = L_\infty(1 - e^{-Ka}) \tag{3}$$

105   The rate at which the numbers-at-age in a population (N) are decreasing can be

106   written as:

$$\frac{dN}{da} = -ZN \tag{4}$$

107   where Z is the instantaneous total mortality rate. The rate of change of numbers alive with

108   respect to length can be written using the chain rule as:

$$\frac{dN}{dL} = \frac{dN}{da}\frac{da}{dL} \tag{5}$$

109   where $\frac{da}{dL}$ is the inverse of the von Bertalanffy growth equation (Equation 3):

$$\frac{da}{dL} = \frac{1}{K(L_\infty - L)} \tag{6}$$

5

110   This gives:

$$\frac{dN}{dL} = -\frac{Z}{K}\frac{N}{(L_\infty - L)} \qquad (7)$$

111   which demonstrates that, on a per-recruit basis, the $\frac{Z}{K}$ ratio determines the number of

112   animals at length. By applying a separation of variables method Equation 7 can be re-

113   arranged as:

$$\frac{dN}{N} = -\frac{Z}{K}\frac{1}{(L_\infty - L)}dL \qquad (8)$$

114   which, by integrating both sides of the equation, gives:

$$\ln N_L = \frac{Z}{K}\ln(L_\infty - L) + C \qquad \text{for } L < L_\infty \qquad (9)$$

115   Assuming a per-recruit model, the initial condition is $N_{L=0}=1$, which can be used to determine

116   the value of C, and replacing it in Equation 9 gives:

$$\ln N_L = \frac{Z}{K}\ln\left(\frac{L_\infty - L}{L_\infty}\right) \qquad (10)$$

117   Exponentiation of Equation 10 results in:

$$N_L = \left(\frac{L_\infty - L}{L_\infty}\right)^{\frac{Z}{K}} \qquad (11)$$

118   It follows that the number-per-recruit that are alive at $L + dL$ (where dL is a small increment

119   in length) is:

$$N_{L+dL} = \left(\frac{L_\infty - L - dL}{L_\infty}\right)^{\frac{Z}{K}} \qquad (12)$$

121   Re-arranging these equations gives:

$$N_{L+dL} = N_L\left(\frac{L_\infty - L - dL}{L_\infty - L}\right)^{\frac{Z}{K}} \qquad \text{for } L < L_\infty \qquad (13)$$

122   This simple recursive equation demonstrates that the number per-recruit that are alive

123   at each length (L) can be determined by the $\frac{Z}{K}$ ratio and the L_∞ parameter.

124   *Including size-dependent mortality*

125   Equation 13 assumes that total mortality is independent of size, and that the Z/K ratio

126   remains constant for all size classes. The total mortality rate is usually separated into two

127   sources: fishing mortality (F) which is imposed by the fishing activity, and natural mortality

128   (M) which generally includes all sources of mortality not associated with the fishing. Fishing

129   mortality is often size dependent, with small individuals often less likely to be vulnerable to

6

130   the fishing gear and selected by the fishery than larger fish. The fishing mortality at size L

131   can be described as:

$$F_L = FV_L \tag{14}$$

133   where F is the fully selected fishing mortality, and V_L is the vulnerability of an individual at

134   length L. Assuming a logistic selectivity curve V_L is given by:

$$V_L = \frac{1}{1 + e^{\left(-\ln(19)\left[\frac{L - S_{L50}}{S_{L95} - S_{L50}}\right]\right)}} \tag{15}$$

135   where S_{L50} and S_{L95} are the lengths at which 50% and 95% of the fish are vulnerable

136   respectively. Other selectivity patterns, e.g., dome-shaped or knife-edge, can easily be

137   incorporated by modifying Equation 15.

138   Total mortality at length is then given by:

$$Z_L = F_L + M_L \tag{16}$$

139   where M_L is the natural mortality rate at length L. Natural mortality is notoriously difficult to

140   estimate, and many stock assessment and bio-energetic models assume that this rate is

141   constant for all ages and size classes. However, there is evidence that natural mortality is

142   higher for smaller individuals, and tends to decrease as the animals grow to larger sizes (with

143   a possible increase again towards the end of life; Charnov et al. 2013, Charnov 2014). This

144   relationship can be described by:

$$M_L = M_{L_\infty} \left(\frac{L_\infty}{L}\right)^c \tag{17}$$

145   where M_{L_∞} is the natural mortality rate for adults near maximum size, and $c \geq 0$ is the

146   allometric exponent for the mortality-length relationship (Lorenzen 1996, 2000).

147   If the length increment dL is small enough, it may be reasonable to assume that both

148   the natural and fishing mortality rates are constant within a size class. This assumption

149   allows size-specific mortality rates to be incorporated into Equation 13:

$$N_{L+dL} = N_L \left(\frac{L_\infty - L - dL}{L_\infty - L}\right)^{\frac{Z_L}{K}} \quad \text{for } L < L_\infty \tag{18}$$

150   *Prediction of size composition*

151   Equation 18 can be used to calculate the number-per-recruit that survive to each

152   length class given a size-dependent mortality rate. However, as the rate of growth tends to

153   decrease as fish get older, the amount of time an individual spends in each length class

154   changes throughout its life; that is, the time to grow from L to $L+dL$ typically increases for

155   older age classes. Therefore, to calculate the expected per-recruit number-at-length within

7

156 each length class, it is necessary to integrate over the amount of time the animal spends in

157 each size class.

158   The age at length L can be calculated by re-arranging Equation 3 to give:

$$a = -\frac{1}{K}\ln\left(1 - \frac{L}{L_\infty}\right) \tag{19}$$

159 To calculate the numbers at age over each length interval we must integrate the number-at-

160 length (N_L) over the increment in age within the length interval:

$$D_{L+dL} = \int_{-\frac{1}{K}\ln\left(1-\frac{L}{L_\infty}\right)}^{-\frac{1}{K}\ln\left(1-\frac{L+dL}{L_\infty}\right)} e^{-Za}\, da \tag{20}$$

161 where D_{L+dL} is the cumulative 'density' of animals between the length classes L and $L+dL$.

162 Solving this equation and simplifying gives:

$$D_{L+dL} = \frac{1}{Z}(N_L - N_{L+dL}) \tag{21}$$

163   Similar to the situation described above, if we assume that dL is small enough so that

164 the mortality rate is constant within the length class, the above equation can be modified to

165 account for size-dependent mortality:

$$D_{L+dL} = \frac{1}{Z_L}(N_L - N_{L+dL}) \tag{22}$$

166 As it is a per-recruit model, Equation 22 can be standardized to sum to one across the length

167 classes:

$$\widetilde{D}_{L+dL} = \frac{\frac{1}{Z_L}(N_L - N_{L+dL})}{\sum_L \frac{1}{Z_L}(N_L - N_{L+dL})} \tag{23}$$

168 Equation 23 now predicts the expected proportion of the population in each size class in

169 terms of L_∞, Z and K (see Equation 18) in recursive fashion. However, it can be simplified

170 further to make the predicted proportions depend on the $\frac{Z}{K}$ ratio instead of the specific value

171 of Z. Multiply the numerator and denominator in the right hand side of Equation 23 by K,

172 which leads to:

$$\widetilde{D}_{L+dL} = \frac{\frac{1}{\theta_L}(N_L - N_{L+dL})}{\sum_L \frac{1}{\theta_L}(N_L - N_{L+dL})} \tag{24}$$

8

173   where θ_L is the ratio $\frac{Z_L}{K}$, enabling the expected per-recruit size composition to be constructed

174   in terms of just L_∞ and $\frac{Z_L}{K}$.

175

176   *Growth-Type-Group Model*

177   The model so far assumes a single growth trajectory for all individuals in the

178   population, and does not account for individual variation in growth. One way to incorporate

179   variability in growth would be to assume that Equation 18 describes the mean length, and

180   that individuals are randomly distributed (e.g., Gaussian distribution) around this mean

181   length. This approach would essentially be identical to the age-structured LBSPR model

182   (Hordyk et al. 2015b, 2015c), which assumed individuals were normally distributed around a

183   mean length-at-age. However, a shortcoming of this approach is that it fails to adequately

184   account for the cumulative effects of size-based fishing mortality on the size structure of the

185   stock, although admittedly some form of truncation could be adopted within this simple

186   statistical approach. Here we develop a more biologically-oriented methodology based on

187   the concept of growth-type-groups.

188   To account for size-dependent fishing mortality, one option is that the population

189   model keeps track of the cumulative fishing mortality rates on several groups of individuals

190   with assumed different growth patterns within a single cohort. These growth-type groups are

191   similar to the super-individual concept in individual-based models (Scheffer et al 1995),

192   although the growth-type groups are simpler to implement. Here we tackle Lee's

193   Phenomenon within the LB-SPR model by recourse to the concept of growth-type-groups

194   (Walters and Martell 2004).

195   To account for variability in individual growth patterns, we assumed that there are G

196   sub-cohorts, and each growth-type-group g has a different L_∞ $(L_{\infty,g})$ but a shared K

197   parameter. Equation 18 can then be written as:

$$N_{L+dL,g} = N_{L,g} \left(\frac{L_{\infty,g} - L - dL}{L_{\infty,g} - L} \right)^{\frac{Z_{L,g}}{K}} \quad \text{for } L < L_{\infty,g} \tag{25}$$

198   and Equation 24 as:

$$\widetilde{D}_{L+dL,g} = \frac{\frac{1}{\theta_L}\left(N_{L,g} - N_{L+dL,g}\right)}{\sum_L \frac{1}{\theta_L}\left(N_{L,g} - N_{L+dL,g}\right)} \tag{26}$$

199

9

200   The initial condition for Equation 25 is:

$$N_{L=0,g} = R_0 p_g \qquad (27)$$

201   where $R_0 = 1$ for a per-recruit model, and, assuming that $L_{\infty,g}$ is normally distributed across

202   the growth-type-groups, p_g is the fraction of recruits to group g and is proportional to a

203   normal probability density function with mean $\bar{L}_\infty$ and variance $\sigma_{L_\infty}^2$.

204   The expected length structure of the stock can then be constructed by summing across

205   the G growth-type-groups the number of individuals in each length class:

$$\ddot{D} = \left\{ \sum_1^G \widetilde{D}_{L+dL,g} \right\}_{L \in [0, L_{\infty,g}]} \qquad (28)$$

206

The Spawning Potential Ratio

208   The length-based growth-type-group model described above can be used to calculate

209   the spawning potential ratio (SPR). The length-weight relationship is often described by

210    $W_L = aL^b$, where a is a species-specific constant, and the exponent b is often close to 3.

211   Maturity-at-size (Mat_L) can be modelled as a logistic function following Equation 15, by

212   replacing S_{L50} and S_{L95} with the average length at 50% ($\bar{L}_{50}$) and 95% ($\bar{L}_{95}$) maturity

213   respectively. To account for the variable growth trajectories, the relative size-at-maturity is

214   assumed to be constant across all GTG, with cohorts with smaller and larger asymptotic sizes

215   reaching maturity at smaller and larger absolute lengths respectively. The size-at-maturity

216   for each growth-type-group is then given by:

$$L_{50,g} = \frac{\bar{L}_{50}}{\bar{L}_\infty} L_{\infty,g}$$
$$L_{95,g} = \frac{\bar{L}_{95}}{\bar{L}_\infty} L_{\infty,g} \qquad (29)$$

217   where $\bar{L}_{50}$ and $\bar{L}_{95}$ are the mean length at 50% and 95% maturity respectively. Equation 15

218   is then used to calculate the maturity schedule for each GTG.

219   Assuming that egg production is proportional to the size of mature fish, relative

220   fecundity-at-size is given by:

$$\text{Fec}_{L,g} = \text{Mat}_{L,g} L^\beta \qquad (30)$$

221   The value of the exponent β in Equation 30 can be changed to reflect different size-

222   fecundity relationships. For example, setting β to zero assumes that the reproductive output

223   of mature individuals is constant and independent of size, perhaps more appropriate for some

224   sharks and other elasmobranchs.

10

225   The SPR can be calculated using the above equations, as the proportion of

226   reproduction in the fished state relative to the unfished state:

$$\text{SPR} = \frac{\sum_g \sum_L \frac{1}{(M_{L,g} + F_L)} (\widetilde{D}_{L,g} - \widetilde{D}_{L+dL,g}) \text{Fec}_L}{\sum_g \sum_L \frac{1}{M_{L,g}} (\widetilde{D}_{L,g} - \widetilde{D}_{L+dL,g}) \text{Fec}_L} \tag{31}$$

227   As was done when passing from Equation 23 to Equation 24, multiply the numerator

228   and denominator on the right hand side of Equation 31 by K. In addition, multiply the $\frac{F_L}{K}$

229   term in the numerator by $\frac{M}{M}$, to get:

$$\text{SPR} = \frac{\sum_g \sum_L \frac{1}{\left(\left[\frac{M}{K}\right]_{L,g} + V_L \left[\frac{F}{M}\right]\left[\frac{M}{K}\right]_{L,g}\right)} (\widetilde{D}_{L,g} - \widetilde{D}_{L+dL,g}) \text{Fec}_L}{\sum_g \sum_L \frac{1}{\left[\frac{M}{K}\right]_{L,g}} (\widetilde{D}_{L,g} - \widetilde{D}_{L+dL,g}) \text{Fec}_L} \tag{32}$$

230   **Growth-Type-Group Length-Based SPR Assessment Model**

231   Assuming reasonable estimates of the M/K ratio, L_∞ and $\sigma^2_{L_\infty}$ (or CV_{L_∞}), size-at-

232   maturity, the parameters F/M, S_{L50}, and S_{L95} can be estimated from a representative sample

233   of the length structure of the catch, by minimizing the following multinomial negative log-

234   likelihood function (NLL):

$$\text{NLL} = \underset{\frac{F}{M}, S_{L50}, S_{L95}}{\text{argmin}} \sum_i O_i \ln \frac{\widetilde{P}_i}{\widetilde{O}_i} \tag{33}$$

235   where O_i and $\widetilde{O}_i$ are the observed number and proportion in length class i respectively, and $\widetilde{P}_i$

236   is the model estimate of the probability in length class i. $\widetilde{P}$ can be calculated by multiplying

237    $\ddot{D}$ from Equation 28 by the estimated selectivity curve, and standardized to sum to one. The

238   spawning potential ratio can be calculated from Equation 32 using the model estimates of

239   F/M and selectivity-at-length parameters, and the input parameters M/K, L_∞ and CV_{L_∞}, and

240   size-at-maturity parameters (Table 1).

241   This new model, referred to as the growth-type-group length-based SPR (GTG LB-

242   SPR), model shares many of the assumptions of the LB-SPR model (Hordyk et al. 2015b,

243   2015c), including the typical per-recruit model assumption that the stock is in steady state,

244   and that growth patterns are static and adequately described by the von Bertalanffy equation.

245   While the model can account for size-dependant natural mortality and dome-shaped

246   selectivity curves, these phenomena are difficult to identify from size data alone. Therefore,

247   the default assumption of the model is that natural mortality is constant for all size classes (at

11

248   least those observed in the catch) and that the selectivity curve is asymptotic. If information

249   exists to estimate the size-dependent natural mortality relationship or selectivity pattern, this

250   information can be incorporated into the model.

251

252   **Simulation and Evaluation of the GTG LB-SPR Model**

253   A simulation framework was used to examine the effect of the different parameters of

254   the GTG LB-SPR model to the predicted size distribution. We also generated size data from

255   both the GTG LB-SPR and the LB-SPR models, and applied the two estimation models to the

256   simulated data sets to evaluate the impact of accounting for and ignoring Lee's Phenomenon.

257   All simulation was conducted using the statistical programming language R (R Core Team

258   2015), and the R code for the simulation and estimation models is available on the lead

259   author's GitHub account (https://github.com/AdrianHordyk/GTG_LBSPR).

260

261   *Life History Parameters*

262   Previous work has demonstrated that the expected unfished size distribution is

263   dependent primarily on the *M/K* ratio, with L_∞ working effectively as a scaling parameter

264   (Hordyk et al. 2015b, Prince et al. 2015b). Although the *M/K* ratio for fish stocks is often

265   assumed to be around 1.5, Prince et al. (2015a) demonstrated that this ratio is much more

266   variable in fish stocks, and ranges from around 0.5 to above 3.0. Values of *M/K* around 1.5 –

267   2.0 and lower appear to be most common (Prince et al. 2015b), and consequently we

268   examined a range of *M/K* ratios (0.5, 1.0, 1.5 and 2.0) in the simulations, but used generic

269   default values for the other life history parameters (Table 1). The population L_∞ was fixed at

270   100, in arbitrary units, and the coefficient of variation in asymptotic length $\left(CV_{L_\infty}\right)$ set to 0.1.

271   Selectivity-at-length was assumed to be equal to length-at-maturity, which was set at 50 and

272   55 for L_{50} and L_{95} respectively. The generated length data was binned into classes of width

273   (*dL*) 5, in the same units as L_∞ and represents a measurement resolution of 5% of asymptotic

274   length. The life history parameters were systemically adjusted from these default values in

275   the specific simulation tests.

276

277   *Evaluation of model behaviour*

278   The GTG LB-SPR model is based on the same principles as the LB-SPR model, and

279   requires the same input parameters: *M/K*, L_∞, CV_{L_∞}, L_{50} and L_{95}. The underlying population

280   dynamics of the two models is essentially the same, with the extra addition of the growth-

281   type-groups to deal with Lee's Phenomenon. Therefore, the new GTG LB-SPR model is

282   expected to display similar sensitivities to misspecification in the input parameters and

283   violations of the assumptions of the model (Hordyk et al. 2015c). However, the new model

284   introduces an extra parameter which needs to be specified, the number of growth-type-

285   groups. We used simulation to evaluate the effect of this parameter on the equilibrium length

286   structure generated by the GTG LB-SPR model.

287

288   *Number of growth-type-groups*

289   The number of growth-type-groups (G) determines the value of the individual $L_{\infty,g}$

290   parameters. For example, in the extreme case of $G=1$, the model would only include a single

291   group and account for no variation in length-at-age. Variability could be added by assuming

292   a probability distribution of length-at-age around this single group. However, the model

293   would then be essentially identical to the LB-SPR model and not account for Lee's

294   Phenomenon.

295   Increasing the number of sub-cohorts increases the resolution of the generated length

296   data, by dividing the different growth trajectories of the model into finer increments; i.e.,

297   smaller increments between the individual $L_{\infty,g}$ of the groups (ΔL_∞). However, the increased

298   number of sub-cohorts also increases the computational requirements of the model. A trade-

299   off exists in determining the number of growth-type-groups which can adequately generate a

300   smooth size composition, without unnecessarily consuming excess computing power.

301   We examined the effect of G on the size distribution predicted by the model. Fewer G

302   was expected to decrease the resolution of the model and result in an increasingly irregular

303   size distribution. The relationship between G and ΔL_∞ is given by:

$$G = \left\lceil \frac{2\lambda\sigma_{L_\infty} + 1}{\Delta L_\infty} \right\rceil \qquad (34)$$

304   where G is rounded up to the nearest integer, and λ is the maximum deviation in units of σ_{L_∞}

305   from $\bar{L}_\infty$ for the smallest and largest group-type-groups (fixed at 2 in these simulations). We

306   assumed a maximum simulation resolution of $\Delta L_\infty = 1$, which represents 41 growth-type-

307   groups with L_∞ ranging from 80 to 120. We systemically varied G under a range of different

308   life-history and fishing mortality conditions, and compared the resulting size composition

309   with that obtained at maximum resolution ($G=41$).

310

311 *Size-dependent natural mortality*

312   The default value of the size-dependent natural mortality parameter (c) was set at 0

313 for the simulations, representing constant natural mortality for all size classes (Table 1). The

314 impact of variation of this parameter on the expected unfished size distribution was examined

315 by running the model with a range of values of c: the base case $c=0$, and $c=0.1$, 0.2 and 0.3,

316 and the four different values of *M/K* (Table 1).

317

318 *Comparison of LB-SPR models*

319   One of the key issues of the model presented in Hordyk et al. (2015c) was that it did

320 not account for the cumulative effect of fishing mortality on the expected length structure of

321 the stock. As a result, the model is expected to estimate higher fishing mortality, and lower

322 SPR, for a given size structure compared to a model that appropriately accounts for Lee's

323 Phenomenon. We compared the estimates of the LB-SPR model, as described by Hordyk et

324 al. (2015c), with the GTG LB-SPR model presented in this paper by applying the two models

325 to both simulated and empirical data.

326   Four sets of equilibrium size distributions, representing the four different life history

327 types (Table 1), were generated with both the LB-SPR model (Hordyk et al. 2015b, 2015c)

328 and the GTG LB-SPR model. Each set contained twenty simulated size composition data

329 with fishing mortality ranging from 0.1 to 3.0. Each estimation model was applied to the

330 dataset generated from the other model, and the resulting bias in estimated parameters was

331 examined. Natural mortality was assumed be constant for all size classes (i.e., c = 0; Table

332 1). All input parameters of the estimation models were fixed at the true values.

333   Recently Prince et al. (2015b) applied the LB-SPR method to twelve tropical reef

334 species from northern Palau. These species are known to be heavily fished in the region,

335 however little biological data exists for local stocks, and few assessments or estimates of the

336 status of these stocks have been conducted previously. Here we applied both the LB-SPR

337 and the GTG LB-SPR models to the four datasets with the largest sample size (n>400), and

338 compared the resulting estimates of *F/M* and SPR. The four species were *Hipposcarus*

339 *longiceps*, *Lutjanus gibbus*, *Lethrinus rubrioperculatus*, and *Variola louti*.

340   Although little biological data exists for these species in Palau, based on the literature

341 for these and related species Prince et al. (2015b) estimated likely ranges for the biological

342 parameters required for the LB-SPR model, and accounted for the uncertainty in these

343 parameters with Monte Carlo simulation.   As the purpose of the current exercise was to

344   compare the results of the two models (with and without accounting for Lee's Phenomenon),

345   we fixed the input parameters of the estimation model at the best estimates determined by

346   Prince et al. (2015b), and compared the resulting point estimates (Table 2).

347

348   **Results**

349   **Simulation Tests**

350   Figure 1 shows the von Bertalanffy growth curves for each sub-cohort, and the

351   resulting equilibrium size composition, when the number of growth-type-groups (G) was set

352   to 41, 9 and 5 for the four values of the M/K ratio: 0.5, 1.0, 1.5, and 2.0. Reducing the value

353   of G from the highest resolution ($G = 41, \Delta L_\infty = 1$) did not significantly affect the quality of

354   the generated size composition until G was about 7 or lower. The life histories with lower

355   M/K ratios were most sensitive to the number of growth-type-groups. For example, Figure

356   1a-d shows the von Bertalanffy growth curves of each sub-cohort, and the resulting size

357   composition when G was set to 41, 9 and 5 and M/K =0.5. The large number of growth-type-

358   groups used in the highest resolution case (G=41; Figure 1a) generated a smooth equilibrium

359   size composition (grey bars in Figure 1d). There was virtually no distinguishable difference

360   in the size composition that was generated when G was reduced to nine (Figure 1b and solid

361   line in Figure 1d). However, a further reduction to $G = 5$, resulted in a highly serrated size

362   structure, as the resolution of the model was too coarse to adequately represent the

363   continuous size composition (Figure 1c and dashed line in Figure 1d).

364   The impact of a lower value for G was less severe for the simulations with M/K=1.0,

365   although the size composition generated when G=5 was slightly deformed compared to that

366   produced when G=41 (Figure 1h dashed line and grey bars respectively). However, the size

367   composition generated with nine growth-type-groups was very similar to that produced when

368   G=41 (Figure 1h solid line and grey bars respectively. The number of growth-type-groups

369   had the least impact on the simulations with the higher values of M/K, where the generated

370   size compositions were effectively identical under a wide range of values of G (Figure 1i-l

371   and Figure 1m-p for M/K=1.5 and 2.0 respectively).

372   Sensitivity to this result was examined by re-running the model with different values

373   of mean L_∞ as well as increased values of CV_{L_∞}, however the general pattern was consistent.

374   There was no discernible reduction in the quality of the size composition when the step size

375   of L_∞ between the growth-type-groups (ΔL_∞) was less than or equal to the width of the

376   length class (dL) into which the length data was binned. For the remainder of the

                                                                                                        15

377   simulations we set $\Delta L_\infty = 0.5dL$. With the parameters used in these simulations ($CV_{L_\infty} =$

378   0.1 and $dL = 5$; Table 1), this resulted in seventeen growth-type-groups (Equation 34).

379   Figure 2 demonstrates the effect of size-dependent natural mortality on the

380   equilibrium unfished size composition for the four values of M/K (Figure 2a, b, c and d

381   respectively) and increasing values of size-dependent M ($c = 0, 0.1, 0.2$ and 0.3). In the base

382   case, natural mortality was constant ($c = 0$) for all individuals, with the resulting size

383   composition equivalent to that predicted by the age-structured LB-SPR model (Prince et al.

384   2015b) for the different values of M/K (Figure 2 solid black lines). Increasing the natural

385   mortality (specifically M/K in this model) for the smaller size classes by increasing the value

386   of c resulted in the smaller individuals contributing proportionally more to the population

387   (Figure 2 dashed, dotted and dash-dotted lines for $c = 0.1, 0.2$, and 0.3 respectively). This

388   effect was especially noticeable for the higher M/K where the size-dependent natural

389   mortality changed the shape of the expected size distribution considerably (Figure 2 bottom

390   row).

391   To investigate the effect of size-dependent natural mortality on the expected size

392   structure of the catch, the model was re-run for the four different life-history parameters at a

393   level of fishing mortality that resulted in SPR=0.5 (Figure 3a, b, c and d for $M/K = 0.5, 1.0$,

394   1.5, and 2.0 respectively). The influence of size-dependent natural mortality on the expected

395   size structure of the catch was effectively indistinguishable under these simulations. It was

396   hypothesised that the impact of size dependent mortality on the size composition of the catch

397   would be more significant when the selection pattern of the fishery included more of the

398   smaller size classes. This was investigated by setting the parameters of the selectivity curve

399   to smaller values (S_{L50} and S_{L95} set at 10 and 15 respectively) and re-running the model with

400   the four different scenarios of size-dependent natural mortality and four sets of life-history

401   parameters (Figure 4). As expected, the effect of the size-dependent mortality was more

402   noticeable in the size structure of the catch under these conditions. This was especially the

403   case for the higher M/K simulations, where the expected size structure of the catch consisted

404   of a proportionally greater number of smaller sized individuals and with increased size-

405   dependent natural mortality (Figure 4c and d).

406

407   **Simulation and Empirical Comparison of Estimation Models**

408   The LB-SPR assessment model over-estimated the fishing mortality when it was

409   applied to length data generated with the growth-type-group model (Figure 5a). This bias

16

410   was especially noticeable at higher levels of fishing mortality ($F/M > 1$) and higher values of

411   the M/K ratio (dotted and dash-dotted lines in Figure 5a). The over-estimation of fishing

412   mortality resulted in a negative bias in the estimated SPR, especially at higher levels of

413   fishing mortality (Figure 5c). However, due to the asymptotic relationship between fishing

414   mortality and SPR, the negative bias in SPR was less pronounced than the positive bias in the

415   fishing mortality.

416   The reverse pattern was observed when the GTG LB-SPR assessment model was

417   applied to length data generated with the assumption of age-based selectivity (i.e., Lee's

418   Phenomenon is not occurring). Because of the assumption of Lee's Phenomenon built into

419   the GTG LB-SPR model, the assessment model expects the size distribution to truncate under

420   lower levels of fishing mortality. Here the assessment model tended to under-estimate the

421   fishing mortality, especially at higher levels of fishing mortality (Figure 5b). Likewise, the

422   GTG LB-SPR model over-estimated the SPR of the stock over the entire range (Figure 5d).

423   The bias was most pronounced at lower levels of SPR and higher values of M/K (Figure 5d).

424   A similar relationship between the two estimation models was observed with the four

425   empirical data sets, with the GTG LB-SPR model consistently estimating values of F/M that

426   were between 65% and 85% of those estimated by the LB-SPR model (Table 2). Likewise,

427   the GTG LB-SPR model estimated a higher level of SPR for all four species, compared to the

428   results of the LB-SPR model (Table 2). This was especially the case for *L. rubrioperculatus*,

429   where the GTG LB-SPR model estimated SPR=0.39, while the LB-SPR model estimated

430   SPR=0.26. The estimated fishing mortality was much higher for the other three species, and

431   the differences in estimated SPR between the two models was much less pronounced. The

432   estimates of the selectivity parameters were very similar between the two models, although

433   the GTG LB-SPR model tended to estimated selectivity parameters that were slightly lower

434   than those from the LB-SPR model.

435

436   **Discussion**

437   The model developed in this study simplifies and improves the LB-SPR model

438   described by Hordyk et al. (2015b, 2015c) to estimate the relative fishing mortality (F/M), the

439   selectivity-at-length parameters, and the SPR of an exploited stock from representative size

440   composition data and assumed known biological parameters. In particular, by using the

441   growth-type-group approach, and splitting the population into a number of separate sub-

442   cohorts, this model accounts for the effect of size-dependent fishing mortality on the size

17

443   structure of the stock (Walters and Martell 2004). Furthermore, by using a length-structured

444   model to generate the expected equilibrium size composition, the GTG LB-SPR model

445   circumvents the complexities of the generic and scaleless age-structured approach used

446   previously (Hordyk et al. 2015b, 2015c).

447   Many age-structured population models that are commonly used in stock assessment

448   assume that all individuals share the same mean growth curve with some variance in size-at-

449   age. These models ignore the effects of size-based fishing mortality on the age and size

450   structure of the stock. The inclusion of growth-type-groups arguably improves model

451   realism, and this idea has been incorporated into several other age-based and length-based

452   assessment models. For example, Sullivan et al. (1990) use a length-based model that

453   accounts for the effects of size dependent mortality by tracking the abundance in each length

454   class. Both Stock Synthesis and CASAL allow for the presence of growth groups (called

455   'morphs' or 'platoons' in Stock Synthesis (Methot and Wetzel, 2013) and 'growth paths' in

456   CASAL (Bull et al. 2012)). In these models, the size-at-age of each sub-cohort, or growth

457   group, is assumed to follow a statistical distribution (e.g., Taylor and Methot, 2013).

458   McGarvey et al. (2007) describe a 'cohort slicing' method, where the normal distribution of

459   length-at-age is sliced into several sub-cohorts, and abundance is tracked for each sub-cohort.

460   The GTG LB-SPR model is similar to the McGarvey et al. (2007) approach in that the

461   growth-type-groups are an intrinsic, rather than optional, part of the model. However, apart

462   from the presence of the growth-type-groups, the GTG LB-SPR model is essentially identical

463   to the LB-SPR model, which does not account for Lee's Phenomenon.   Lee's Phenomenon

464   will only occur when selectivity is size-based, and it is important to note that the GTG LB-

465   SPR model assumes that all biological and fishery processes are size- rather than age-

466   dependent. Selectivity processes in fisheries are generally thought to be primarily size-

467   dependent, but there are scenarios where this assumption is likely to be violated. For

468   example, species that have an ontogenetic migration may be better described by age-based

469   selectivity, or a combination of the two (Punt et al. 2013, Francis 2015).

470   The new GTG LB-SPR model and the original LB-SPR model were compared by

471   applying both models to simulated data, and length data from four reef fish species from

472   Palau in the western Pacific (Prince et al. 2015a). These results demonstrate the GTG LB-

473   SPR model consistently estimates a lower relative fishing mortality (F/M) and higher SPR

474   compared to the LB-SPR model. The difference between the two models was greatest at

475   higher levels of fishing mortality, and more pronounced in the estimates of F/M than the

476   estimates of SPR. If selectivity is actually size-based, these results suggest that ignoring

18

477   Lee's Phenomenon is likely to result in over-estimates of fishing mortality by about 15%.

478   Conversely, if size-based selectivity is assumed where in fact it is not occuring, the

479   assessment model is likely to under-estimate the fishing mortality. While the GTG LB-SPR

480   model consistently estimated lower F/M values, the difference between the two methods was

481   relatively minor. In the data-limited situations where these methods could be applied,

482   researchers may prefer the more conservative estimates of the LB-SPR model unless there

483   was sufficient evidence that selectivity was primarily a function of size.

484   The bias is less severe in the estimates of the spawning potential ratio. At low levels

485   of fishing mortality, the presence (or absence) of size-based fishing mortality has little impact

486   on the size structure of the stock. At high levels of fishing mortality, the non-linear

487   asymptotic relationship between fishing mortality and SPR means that, although the estimate

488   of fishing mortality may be biased, there is only a marginal difference in SPR. This suggests

489   that accounting for Lee's Phenomenon is most important when directly using the estimate of

490   fishing mortality (or F/M) that is produced by the model, for example to determine

491   appropriate catch recommendations. In situations where it is not clear whether selectivity is

492   predominantly size-based or age-based, we suggest applying both the GTG LB-SPR and the

493   LB-SPR models, and evaluating the magnitude and significance of the difference in results.

494   The GTG LB-SPR model belongs in the per-recruit family of methods and is based on

495   the same principles as the LB-SPR model (Hordyk et al. 2015b, 2015c). The new model

496   shares many of the same behaviours as the LB-SPR model, including sensitivities to miss-

497   specification in the life history parameters (especially L_∞) and violations to the equilibrium

498   assumption (Hordyk et al. 2015c). The sensitivity to non-equilibrium conditions is common

499   to all per-recruit methods, and the equilibrium assumption is likely to be often violated

500   (Hilborn and Walters, 1992). Hordyk et al. (2015a) examined the effects of non-equilibrium

501   dynamics on the estimates of the LBSPR model and found that, although unbiased on

502   average, individual estimates of SPR could at times vary considerably from the true values.

503   Averaging length data over a number of years, particularly for short lived species, may be an

504   effective way to mitigate this issue (Punt et al. 2013). Furthermore, recent work has shown

505   that if a stock is out of equilibrium primarily due to the effect of fishing, an iterative effort-

506   based control rule based on the LB-SPR method can still be effective in incrementally

507   adjusting fishing pressure until the SPR and size structure of the stock stabilises around target

508   levels (Hordyk et al. 2015a). The equilibrium assumption may also be dealt with by

509   incorporating a time series of length composition data, as well as estimates of recent

510   recruitment trends. However, such a model would also necessarily require some estimate of

19

511   the time-scale of the species, (e.g. natural mortality and growth rates) which is more data

512   intensive then the method presented here.

513   While the growth-type-group approach could be incorporated into a fully dynamic

514   model, the simple recursive equations of the length-structured model developed here would

515   no longer apply. In a dynamic model, the abundance of animals in each length class is no

516   longer determined solely by the abundance in the previous length class, and the growth and

517   mortality patterns, but also by year-to-year variation in recruitment and other sources in inter-

518   annual variability. For example, the dynamic model could track the impact of time-varying

519   natural mortality, selectivity, or growth patterns. An age-structured model could be

520   developed which tracks abundance in a number of growth-type-groups in a similar manner to

521   that done in the GTG LB-SPR model: numerous growth-type-groups, each with their own

522   von Bertalanffy growth curve, and annual recruitment distributed across these groups.

523   However, the number of growth-type-groups would have to be much higher in an age-

524   structured model, and the time-step in the age-based model would have to be small enough to

525   adequately model continuous fish growth, especially for life-histories where growth is rapid

526   in the first few years of life. The dynamic, age-structured GTG model would require

527   additional computational power, and further research is required to determine if this approach

528   offers significant advantages over the statistical distribution method used by Stock Synthesis

529   3 and CASAL.

530   Although developed for data-limited situations, where there is limited biological

531   information and possibly only a few years of size data available, the approach developed in

532   the GTG LB-SPR model may still be useful to data-rich stock assessment modelling, and the

533   calculation of biological reference points. For example, the model can be used to evaluate

534   the effect on alternative selectivity patterns on the expected spawning potential ratio of the

535   stock. Furthermore, it is straightforward to include Botsfords' method of integrating per-

536   recruit dynamics and the Beverton-Holt stock-recruitment function, to determine the relative

537   expected yield for a given selectivity pattern and fishing mortality (Botsford and Wickham

538   1979, Botsford 1981a, b, Walters and Martell 2004). This approach allows analysts to

539   incorporate knowledge of the stock-recruitment dynamics into the per-recruit model to

540   evaluate alternative harvest policies in terms of both spawning potential and relative yield.

541   We intend to explore this in future research.

542   The L_∞ and K parameters are frequently assumed to be negatively correlated, and

543   some may believe that ignoring this correlation is a serious shortcoming of the GTG LB-SPR

544   model. However, the negative correlation commonly observed in estimates of these two

20

545   parameters is primarily a result of the estimation process, where the same data can be fitted

546   just as well under a range of values of L_∞ and K (Pilling et al. 1990, Evenson et al. 2007).

547   There appears to be no biological reason why individuals with a lower than average L_∞

548   should have a higher than average K, or vice versa (Evenson et al. 2007). Furthermore, the

549   longitudinal growth data required to estimate this correlation is rarely available for fish stocks

550   (Evenson et al. 2007). Finally, the observed covariation between L_∞ and K is typically based

551   on observations across species and populations, not among individuals within populations.

552   The growth coefficient K represents the metabolic rate, and appears to vary little among

553   individuals in many fish stocks (Sainsbury 1980). Wang and Thomas (1995) hypothesize that

554   L_∞ is genetically determined and thus fixed for individuals throughout their life, while the

555   metabolic rate K is environmentally driven and likely to be shared amongst individuals of a

556   cohort. Simulation studies have demonstrated that, while in reality both parameters are likely

557   to vary amongst individuals, it is generally sufficient to allow variability in individual L_∞

558   while maintaining a shared (possibly time-varying) K for all individuals (Sainsbury 1980;

559   Wang et al 1995; Wang and Ellis 1998; Eveson et al. 2007). The biological drivers behind

560   the variability in individual growth are not well understood, and the topic is an active area of

561   research (see Shelton et al. 2013 and references therein). It is common to account for

562   variable growth by assuming a single K and variable L_∞ in simulation and assessment models

563   (Sainsbury 1980, Wang and Thomas 1995, Wang and Ellis 1998). We followed this same

564   approach in the per-recruit model by assuming that K is shared by all sub-cohorts, and each

565   growth-type-group has an individual L_∞ which is normally distributed around the mean

566   asymptotic length of the population.

567   However, the splitting a population into several growth groups introduces another

568   issue which we believe has not been previously recognized or addressed. Natural mortality is

569   commonly assumed to be constant for all individuals within a cohort. However, the faster

570   growing individuals reach a larger maximum size, and produce considerably more eggs-per-

571   recruit (a proxy for fitness) compared to the slower growing sub-cohorts. This disparity in

572   per-recruit egg production would lead to significant selection pressure towards the faster

573   growing individuals. The persistence of individual variation within a population suggests

574   there is equivalent fitness between these alternative life-history strategies.

575   One hypothesis to balance the fitness between growth-type-groups is for the faster

576   growing groups to experience relatively greater rates of natural mortality than the slower

577   growing groups. The mechanism can be explained as follows. Faster growing groups of

578   individuals must consume greater amounts of food compared to slower growing individuals

579   of the same cohort, and must therefore venture farther for food and expose themselves to

580   higher levels of predation. Conversely, portions of a cohort which stay within the safe habitat

581   may be protected from increased predation risk, but will grow slower due to the decreased

582   availability of food. This issue is further complicated by the fact that natural mortality in fish

583   is often observed to decrease as individuals grow larger (see below). A further complicating

584   factor is that individuals reaching a larger size sooner within the same cohort may find refuge

585   from predation, and therefore experience less natural mortality (Pennings 1990).

586   We modified the GTG LB-SPR model by assuming a linear increase in natural

587   mortality across the growth-type-groups, and used the numerical optimisation routine *optim*,

588   part of the base R package *stats* (R Core Team 2015), to search for the natural mortality

589   pattern which resulted in approximately equal fitness across the GTGs, while maintaining the

590   mean length-at-age of the unfished population following the specified von Bertalanffy growth

591   curve. We compared the shape of the generated size composition both with and without

592   accounting for the differential in fitness, and applied the estimation model to the size data

593   generated under both scenarios. The results of this analysis found that there was very little

594   difference in the resulting estimates of F/M, selectivity parameters and SPR, and this

595   difference is likely to be insignificant compared to the other sources of variability that are

596   likely in an application of this methodology. Varying the natural mortality to ensure fitness-

597   per-recruit is approximately equal across the GTGs is arguably more realistic, but this

598   approach adds considerable extra complexity to the model, and does not significantly impact

599   the results of the estimation model. The biological mechanisms that must exist to maintain

600   individual variability in growth are not well understood. Regardless of the mechanisms

601   involved, evolutionary theory suggests that relative fitness across different sub-cohorts must

602   be approximately equal for individual variability in growth to persist in a population (Mangel

603   et al. 2006). We believe that this is an important area for further research.

604   Life history theory suggests that M is likely to be higher for smaller, younger

605   individuals, and decrease with increasing size (Lorenzen 2000, Andersen and Beyer 2013).

606   However, stock assessment models often do not incorporate age or size-specific mortality

607   directly, perhaps because of the paucity of data for estimating natural mortality rates

608   (Maunder and Punt 2013, Punt et al. 2013, Prince et al. 2015b). Our results demonstrate that

609   the presence of size-specific M has a direct impact on the shape of the expected unfished size

610   composition. The effect is less significant on the expected size structure of the catch,

611   especially if fishing mortality is significant and the fishery targets only relatively large

22

612   individuals. There are fisheries where juveniles and small individuals contribute to a

613   significant proportion of the catch; e.g., tuna fisheries, where M is known to be size-

614   dependent and fisheries often target juveniles (Hampton 2000). The GTG LB-SPR allows the

615   flexibility of including size-dependent M, and sensitivity to this parameter should be explored

616   when applying the model to empirical data.

617   Evaluating the uncertainty caused by poorly known biological parameters is also

618   important. A reliable estimate of the asymptotic size of the species is critical for reliable

619   estimates of the fishing mortality and SPR. These biological parameters are likely to be

620   poorly known, especially in the data-poor situations where such a model may be applied.

621   Monte Carlo simulations with random draws of parameters over a range of likely values is a

622   useful way to capture some of the uncertainty arising from poorly understood biology (Prince

623   et al. 2015a). Incorporating the model into a Bayesian framework, using Markov chain

624   Monte-Carlo sampling, would also be an important development for this methodology, and

625   provide Bayesian measures of uncertainty (Punt and Hilborn 1997, Magnusson et al. 2013).

626   This approach would be particularly advantageous in a data-poor situation, where prior

627   information on the biological parameters can be incorporated into the model. However, a

628   good understanding of the biology of the exploited species is still very important, particularly

629   for the L_∞ parameter. Often the GTG LB-SPR model can fit equally well to the data for a

630   range of different values of L_∞, with considerable variation in the resulting estimates of SPR.

631   In many of the situations where the LB-SPR model would be applied, length-at-age

632   data are not available, and it may not be possible to estimate the growth curve directly for the

633   stock. In such circumstances the life history parameters would have to be 'borrowed' from

634   other stocks or closely related species. This reinforces the critical importance of high quality

635   biological studies of fish stocks, as well as the utility of comparative studies for

636   understanding patterns in life-history and borrowing parameters from other stocks or regions

637   (Prince et al. 2015b).

638   The effect of Lee's Phenomenon of differential cumulative fishing mortality for

639   different sub-cohorts also impacts the estimation of biological parameters. For example, the

640   removal of larger fish from the population is likely to bias the estimated parameters of the

641   growth curve. Figure 6 shows the relative error in the estimated L_∞ and K parameters from

642   fitting a von Bertalanffy growth curve to mean length-at-age data from a simulated

643   population under increasing levels of fishing mortality. As fishing mortality was increased,

644   the L_∞ parameter was consistently under-estimated and the estimates of the K parameter were

645   positively biased.   This was especially the case for species with a high M/K ratio, where

                                                                                          23

646   there are relatively few larger sized individuals even in the unfished state (see Figure 2), and

647   the relative error in L_∞ and K were -0.09 and 0.06 respectively under the highest level of

648   fishing mortality. The bias in the estimates of the growth parameters is likely to be a function

649   of both the fishing mortality, and the selectivity pattern of the fishery. Here, we explored

650   only a simple case with one selectivity pattern. However, these results conform with the

651   findings from more elaborate simulation studies (Vaughan and Burton 1994, Goodyear

652   1995). Data sets from which growth can be estimated are likely to come from conditions

653   where fishing impacts have already substantially affected the size and age structure of the

654   stock. Using negatively biased estimates of the L_∞ parameter in the LB-SPR model can result

655   in substantial over-estimates of the SPR (Hordyk et al. 2015c).

656   When estimates of growth curves exist for a stock, and Lee's Phenomenon has not

657   been taken into account, one approach to address this issue is to iteratively re-fit the GTG

658   LB-SPR model while adjusting the von Bertalanffy growth parameters until the predicted

659   mean length-at-age in the fished state matches that observed in the exploited fishery. For

660   example, the GTG LB-SPR model would first be fitted to the length data with the estimated

661   von Bertalanffy growth parameters. Given the estimated selectivity pattern and fishing

662   mortality, the expected mean length-at-age of the fished population could be calculated from

663   the model. The change in the growth parameters required for the expected mean length-at-

664   age to match that observed in the data could be calculated, and then the model re-fitted with

665   these updated estimates. The process would be repeated until the predicted mean length-at-

666   age matched that observed in the data, and the estimates of *F/M* and SPR remained

667   unchanged. The result of this method would be to back-calculate the von Bertalanffy growth

668   parameters for the stock in the unfished state, and remove the downward bias in the estimated

669   *F/M*.

670

Acknowledgments

678

679   **References**

680   Andersen, K.H., and Beyer, J.E. 2013. Size structure, not metabolic scaling rules, determines
681   fisheries reference points. Fish Fish.: 1–22. doi: 10.1111/faf.12042.

682   Andrew, N.L., Béné, C., Hall, S.J., Allison, E.H., Heck, S., and Ratner, B.D. 2007. Diagnosis
683   and management of small-scale fisheries in developing countries. Fish Fish. **8**: 227–240.
684   doi: 10.1111/j.1467-2679.2007.00252.x.

685   Béné, C. 2003. When Fishery Rhymes with Poverty: A First Step Beyond the Old Paradigm
686   on Poverty in Small-Scale Fisheries. World Dev. **31**: 949–975. doi: 10.1016/S0305-
687   750X(03)00045-7.

688   Bentley, N. 2015. Data and time poverty in fisheries estimation: potential approaches and
689   solutions. ICES J. Mar. Sci. **72**: 186–193.

690   Beverton, R.J.H. 1992. Patterns of reproductive strategy parameters in some marine teleost
691   fishes. J. Fish Biol. **41**: 137–160.

692   Botsford, L. W. (1981a). Optimal fishery policy for size-specific density-dependent
693   population models. Journal of Mathematical Biology **12:** 265–293.
694   doi:10.1007/BF00276917

695   Botsford, L. W. (1981b). The effects of increased individual growth rates on depressed
696   population size. American Naturalist **117**: 38–63. doi:10.1086/283685

697   Botsford, L. W., and Wickham, D. E. (1979). Population cycles caused by inter-age, density-
698   dependent mortality in young fish and crustaceans. Cyclic phenomena in marine plants
699   and animals. In 'Proceedings of the 13th European Marine Biology Symposium', 27
700   September–4 October 1978, Isle of Man, UK. (Eds E. Naylor and R. G. Hartnoll.) pp.
701   73–82. (Permagon: New York.)

702   Bull, B. Francis, R.I.C.C. Dunn, A. McKenzie, A. Gilbert, D.J.; Smith, M.H. Bian, R. Fu, D.
703   (2012). CASAL (C++ algorithmic stock assessment laboratory): CASAL User Manual
704   v2.30-2012/03/21. NIWA Technical Report 135. 275 p.

705   Charnov, E.L. 2014. Gompertz mortality, natural selection, and the "shape of ageing." Evol.
706   Ecol. Res. **16**: 435–439.

707   Charnov, E.L., Gislason, H., and Pope, J.G. 2013. Evolutionary assembly rules for fish life
708   histories. Fish Fish. **14**: 213–224. doi: 10.1111/j.1467-2979.2012.00467.x.

709   Costello, C., Ovando, D., Hilborn, R., Gaines, S.D., Deschenes, O., and Lester, S.E. 2015.
710   Status and solutions for the world's unassessed fisheries. Science. **338**: 517–20. doi:
711   10.1126/science.1223389.

712   Dowling, N.A., Dichmont, C.M., Haddon, M., Smith, D.C., Smith, A.D.M., and Sainsbury,
713   K. 2015. Empirical harvest strategies for data-poor fisheries: A review of the literature.
714   Fish. Res. **171**: 141–153. doi: 10.1016/j.fishres.2014.11.005.

25

715 Erzini, K. 1990. Sample size and grouping of data for length-frequency analysis. Fish. Res. **9**:
716   355–366. doi: 10.1016/0165-7836(90)90053-X.

717 Eveson, J.P., Polacheck, T., and Laslett, G.M. 2007. Consequences of assuming an incorrect
718   error structure in von Bertalanffy growth models: a simulation study. Can. J. Fish.
719   Aquat. Sci. **64**: 602–617. doi: 10.1139/f07-036.

720 Francis, R.I.C.C. 2015. Growth in age-structured stock assessment models. Fish. Res.
721   Elsevier B.V. doi: 10.1016/j.fishres.2015.02.018.

722 Gerritsen, H.D., and McGrath, D. 2006. Precision estimates and suggested sample sizes for
723   length-frequency data. Fish. Bull. **106**: 116–120.

724 Goodyear, C.P. 1995. Mean Size at Age: An Evaluation of Sampling Strategies with
725   Simulated Red Grouper Data. Trans. Am. Fish. Soc. **124**: 746–755.

726 Hampton, J. 2000. Natural mortality rates in tropical tunas: size really does matter. Can. J.
727   Fish. Aquat. Sci. **57**: 1002–1010. doi: 10.1139/f99-287.

728 Heery, E.C., and Berkson, J. 2009. Systematic errors in length frequency data and their effect
729   on age-structured stock assessment models and management. Trans. Am. Fish. Soc. **138**:
730   218–232. doi: 10.1577/T07-226.1.

731 Hilborn, R. 2007. Moving to sustainability by learning from successful fisheries. Ambio **36**:
732   296–303.

733 Hilborn, R., and Ovando, D. 2014. Reflections on the success of traditional fisheries
734   management. ICES J. Mar. Sci. **71**: 1040-1046.

735 Hilborn, R., and Walters, C.J. 1992. Quantitative fisheries stock assessment: choice,
736   dynamics and uncertainty. Chapman and Hall, New York.

737 Honey, K., Moxley, J., and Fujita, R. 2010. From rags to fishes: data-poor methods for
738   fishery managers. *In* Managing Data-Poor Fisheries Workshop: Case Studies, Models
739   and Solutions. California Sea Grant College Program. pp. 159–184.

740 Hordyk, A.R., Loneragan, N.R., and Prince, J.D. 2015a. An evaluation of an iterative harvest
741   strategy for data-poor fisheries using the length-based spawning potential ratio
742   assessment methodology. Fish. Res. **171**: 20–32.

743 Hordyk, A.R., Ono, K., Sainsbury, K.J., Loneragan, N., and Prince, J.D. 2015b. Some
744   explorations of the life history ratios to describe length composition, spawning-per-
745   recruit, and the spawning potential ratio. ICES J. Mar. Sci. **72**: 204–216.

746 Hordyk, A.R., Ono, K., Valencia, S.R., Loneragan, N.R., and Prince, J.D. 2015c. A novel
747   length-based empirical estimation method of spawning potential ratio (SPR), and tests of
748   its performance, for small-scale, data-poor fisheries. ICES J. Mar. Sci. **72**: 217–231.

749 Jardim, E., Azevedo, M., and Brites, N.M. 2015. Harvest control rules for data limited stocks
750   using length-based reference points and survey biomass indices. Fish. Res. **171**: 12–19.
751   doi: 10.1016/j.fishres.2014.11.013.

752 Kelly, C.J., Codling, E.A. 2006. "Cheap and dirty" fisheries science and management in the
753   North Atlantic. Fish. Res. **79**: 233–238. doi: 10.1016/j.fishres.2006.03.007.

754 Kenchington, T.J. 2014. Natural mortality estimators for information-limited fisheries. Fish
755   Fish. **15**: 1–30. doi: 10.1111/faf.12027.

756 Kent, G. 1997. Fisheries, food security, and the poor. Food Policy **22**: 393–404.

757 Kokkalis, A., Thygesen, U.H., Nielsen, A., and Andersen, K.H. 2015. Limits to the reliability
758   of size-based fishing status estimation for data-poor stocks. Fish. Res. **171**: 4–11. doi:
759   10.1016/j.fishres.2014.10.007.

760 Lee, R.M. 1912. An investigation into the methods of growth determination in fishes by
761   means of scales. J Cons Int. Explor Mer. **s1**: 3–34. doi: 10.1093/icesjms/s1.63.3.

762 Lorenzen, K. 1996. The relationship between body weight and natural mortality in juvenile
763   and adult fish: a comparison of natural. J. Fish Biol. **49**: 627–647. doi: 10.1111/j.1095-
764   8649.1996.tb00060.x.

765 Lorenzen, K. 2000. Allometry of natural mortality as a basis for assessing optimal release
766   size in fish-stocking programmes. Can. J. Fish. Aquat. Sci. **57**: 2374–2381. doi:
767   10.1139/f00-215.

768 Magnusson, A., Punt, A.E., and Hilborn, R. 2013. Measuring uncertainty in fisheries stock
769   assessment: The delta method, bootstrap, and MCMC. Fish Fish. **14**: 325–342. doi:
770   10.1111/j.1467-2979.2012.00473.x.

771 Mangel, M., Kindsvater, H.K., and Bonsall, M.B. 2007. Evolutionary analysis of life span,
772   competition, and adaptive radiation, motivated by the Pacific rockfishes (Sebastes).
773   Evolution. **61**: 1208–1224. doi: 10.1111/j.1558-5646.2007.00094.x.

774 Maunder, M.N., and Punt, A.E. 2013. A review of integrated analysis in fisheries stock
775   assessment. Fish. Res. **142**: 61–74.

776 McGarvey, R., Feenstra, J.E., and Ye, Q. 2007. Modeling fish numbers dynamically by age
777   and length: partitioning cohorts into "slices." Can. J. Fish. Aquat. Sci. **64**: 1157–1173.
778   doi: 10.1139/f07-080.

779 Methot, R.D., and Wetzel, C. 2013. Stock synthesis: A biological and statistical framework
780   for fish stock assessment and fishery management. Fish. Res. **142**: 86–99. Elsevier B.V.
781   doi: 10.1016/j.fishres.2012.10.012.

782 Needle, C.L. 2015. Using self-testing to validate the SURBAR survey-based assessment
783   model. Fish. Res. **171**: 78–86. doi: 10.1016/j.fishres.2015.03.001.

27

784   Pennings, S.C. 1990. Predator-prey interactions in opisthobranch gastropods: effects of prey
785   body size and habitat complexity. *Mar. Ecol. Prog. Ser.* **62**: 95–101.

786   Pilling, G.G.M., Kirkwood, G.P., and Walker, S.G. 2002. An improved method for
787   estimating individual growth variability in fish, and the correlation between von
788   Bertalanffy growth parameters. Can. J. Fish. Aquat. Sci. **59**: 424–432.

789   Pitcher, T.J., and Cheung, W.W.L. 2013. Fisheries: Hope or despair? Mar. Pollut. Bull. **74**:
790   506-516. doi: 10.1016/j.marpolbul.2013.05.045.

791   Prince, J.D., Victor, S., Kloulchad, V., and Hordyk, A.R. 2015a. Length based SPR
792   assessment of eleven Indo-Pacific coral reef fish populations in Palau. Fish. Res. **171**:
793   42–58. doi: 10.1016/j.fishres.2015.06.008.

794   Prince, J.D., Hordyk, A.R., Valencia, S.R., Loneragan, N.R., and Sainsbury, K.J. 2015b.
795   Revisiting the concept of Beverton–Holt life-history invariants with the aim of
796   informing data-poor fisheries assessment. ICES J. Mar. Sci. **72**: 194–203.

797   Punt, A.E., and Hilborn, R. 1997. Fisheries stock assessment and decision analysis: the
798   Bayesian approach. Rev. Fish Biol. Fish. **63**: 35–63.

799   Punt, A.E., Huang, T., and Maunder, M.N. 2013. Review of integrated size-structured models
800   for stock assessment of hard-to-age crustacean and mollusc species. ICES J. Mar. Sci.
801   **70**: 16–33. doi: 10.1093/icesjms/fst048.

802   Punt, A.E., Smith, A.D.M., and Cui, G. 2002. Evaluation of management tools for Australia's
803   South East Fishery 1. Modelling the South East Fishery taking account of technical
804   interactions. Mar. Freshw. Res. **53**: 615–629. doi: 10.1071/MF01007.

805   Quinn, T.J., and Deriso, R.B. 1999. Quantitative Fish Dynamics. Oxford University Press,
806   New York.

807   R Core Team. 2015. R: A language and environment for statistical computing. R Foundation
808   for Statistical Computing, Vienna, Austria. Available from www.R-project.org.

809   Roa-Ureta, R.H. 2015. Stock assessment of the Spanish mackerel (*Scomberomorus
810   commerson*) in Saudi waters of the Arabian Gulf with generalized depletion models
811   under data-limited conditions. Fish. Res. **171**: 68–77. doi: 10.1016/j.fishres.2014.08.014.

812   Roa-Ureta, R.H., Molinet, C., Barahona, N., and Araya, P. 2015. Hierarchical statistical
813   framework to combine generalized depletion models and biomass dynamic models in
814   the stock assessment of the Chilean sea urchin (*Loxechinus albus*) fishery. Fish. Res.
815   **171**: 59–67. doi: 10.1016/j.fishres.2014.12.006.

816   Sainsbury, K.J. 1980. Effect of Individual Variability on the von Bertalanffy Growth
817   Equation. Can. J. Fish. Aquat. Sci. **37**: 241–247.

818   Scheffer, M., Baveco, J.M., Deangelis, D.L., Rose, K. a, and Vannes, E.H. 1995. Super-
819   Individuals A Simple Solution For Modeling Large Populations On An Individual Basis.
820   Ecol. Modell. **80**: 161–170. doi: 10.1016/0304-3800(94)00055-M.

28

821 Shelton, A.O., Satterthwaite, W.H., Beakes, M.P., Munch, S.B., Sogard, S.M., and Mangel,
822   M. 2013. Separating intrinsic and environmental contributions to growth and their
823   population consequences. Am. Nat. **181**: 799–814. doi: 10.1086/670198.

824 Sullivan, P.J., Lai, H.-L., and Gallucci, V.F. 1990. A catch-at-length analysis that
825   incorporates a stochastic model of growth. Can. J. Fish. Aquat. Sci. **47**: 184–198. doi:
826   10.1139/f90-021.

827 Taylor, I.G., and Methot, R.D. 2013. Hiding or dead? A computationally efficient model of
828   selective fisheries mortality. Fish. Res. **142**: 75–85. Elsevier B.V. doi:
829   10.1016/j.fishres.2012.08.021.

830 Thorson, J.T., and Cope, J.M. 2015. Catch curve stock-reduction analysis: An alternative
831   solution to the catch equations. Fish. Res. **171**: 33–41. doi:
832   10.1016/j.fishres.2014.03.024.

833 Vaughan, D.S., and Burton, M.L. 1994. Estimation of von Bertalanffy growth parameters in
834   the presence of size-selective mortality: A simulated example with red grouper. Trans.
835   Am. Fish. Soc. **123**: 1–8.

836 Walmsley, S., Purvis, J., and Ninnes, C. 2006. The role of small-scale fisheries management
837   in the poverty reduction strategies in the Western Indian Ocean region. Ocean Coast.
838   Manag. **49**: 812–833. doi: 10.1016/j.ocecoaman.2006.08.006.

839 Walters, C.J., and Martell, S.J.D. 2004. Fisheries ecology and management. Princeton
840   University Press, Princeton, USA.

841 Wang, Y.-G., and Thomas, M. 1995. Accounting for individual variability in the von
842   Bertalanffy growth model. Can. J. Fish. Aquat. Sci. **52**: 1368–1375.

843 Wang, Y.-G., Thomas, M.R., and Somers, I.F. 1995. A maximum likelihood approach for
844   estimating growth from tag–recapture data. Can. J. Fish. Aquat. Sci. **52**: 252–259. doi:
845   10.1139/f95-025.

846 Wang, Y.-G., and Ellis, N. 1998. Effect of individual variability on estimation of population
847   parameters from length-frequency data. Can. J. Fish. Aquat. Sci. **55**: 2393–2401. doi:
848   10.1139/cjfas-55-11-2393.Worm, B., and Branch, T.A. 2012. The future of fish. Trends
849   Ecol. Evol. **27**: 594–9. doi: 10.1016/j.tree.2012.07.005.

850

Figures Captions

852 Figure 1 The individual von Bertalanffy growth curves of simulations with 41, 9 and 5
853 growth-type-groups (G; columns 1, 2 and 3 respectively) and the resulting expected size
854 composition (column 4) with grey bars representing the size structure generated with G=41,
855 solid black line when G=9, and dashed black line when G=5. Panels a-d show the
856 simulations when $M/K = 0.5$, e-h $M/K = 1.0$, i-l $M/K = 1.5$, and m-p $M/K = 2.0$. Due to the
857 small interval between the growth-type-groups, it is not possible to distinguish the 41

858 individual growth curves in column 1. The thick line in columns 2 and 3 represent the central
859 growth-type-group which shares the L_∞ parameter with the population as a whole.
860

861 Figure 2 Simulations from the GTG LB-SPR model showing the expected equilibrium
862 unfished length composition for four different values of M/K (0.5, 1.0, 1.5, and 2.0 for a, b, c,
863 and d respectively) and increasing values of c, the parameter controlling size-dependent
864 natural mortality.
865

866 Figure 3 The expected equilibrium size composition of the catch for a) $M/K = 0.5$, b) 1.0, c)
867 1.5 and d) 2.0, at SPR=0.50, with four different values of size-dependent natural mortality
868 coefficient (solid, dashed, dotted, and dash-dotted lines for c=0, 0.1, 0.2, and 0.3
869 respectively). The differences between the four size-dependant natural mortality rates are
870 almost indistinguishable on the plot. The other life history parameters are shown in Table 1.
871

872 Figure 4 The expected equilibrium size composition of the catch for a) $M/K = 0.5$, b) 1.0, c)
873 1.5 and d) 2.0, at SPR=0.50, and with a smaller size at selectivity (S_{L50} and S_{L95} set to 10 and
874 15 respectively, and with four different values of size-dependent natural mortality coefficient
875 (solid, dashed, dotted, and dash-dotted lines for c=0, 0.1, 0.2, and 0.3 respectively). The
876 differences between the four size-dependant natural mortality rates are more clearly visible in
877 these simulations. The other life history parameters are shown in Table 1.
878

879 Figure 5 The simulated (x-axis) and estimated (y-axis) values of F/M and SPR when the size
880 data was generated with the GTG LB-SPR model and the parameters estimated with the LB-
881 SPR model (panels a and c) and vice versa (panels b and d), for four ratios of M/K (M/K =
882 0.5, 1.0, 1.5 and 2.0 for the solid, dashed, dotted, and dash-dotted lines respectively.
883

884 Figure 6 The relative error in the estimated L_∞ and K parameters when the von Bertalanffy
885 growth equation is fitted to length-at-age data from a population under increasing levels of
886 exploitation. Lee's Phenomenon results in the selective removal of faster growing
887 individuals from the population, which depresses the observed mean length-at-age and results
888 in biased estimates of the growth parameters, especially for the highest M/K species under
889 high fishing mortality.   Four different life history types were examined: $M/K = 0.5, 1.0, 1.5,$
890 and 2.0 (solid, dashed, dotted, and dash-dotted lines respectively). See Table 1 for other
891 biological parameters.

Table 1 The biological, selectivity and other parameters of the growth-type-group model describing the four different life history types that were used in the simulations of the GTG LB-SPR model.

Parameter	Value	Description
Input Parameters		
M/K	0.5, 1.0, 1.5, 2.0	Ratio of natural mortality (M) to the von Bertalanffy K parameter. Four different values represent a range of life-histories commonly observed in fish.
$\bar{L}_\infty$	100	The mean asymptotic length of unfished population.
$CV_{L\infty}$	0.1	Coefficient of variation of L_∞, which defines the variation in asymptotic length across the sub-cohorts in the growth-type-group model.
$\bar{L}_{50}$	50	Mean length at which 50% of the population is mature.
$\bar{L}_{95}$	55	Mean length at which 95% of the population is mature.
β	3	The exponent of the length-fecundity relationship, set to 3 as fecundity assumed to be proportional to weight.
c	0	Exponent of natural mortality-at-length (or M/K at length). Set to 0 (constant M) for most simulations, but examined at 0.1, 0.2, and 0.3.
G	17	Number of growth-type-groups in the model. Default value of 17, but examined at range of different values.
dL	5	Width of the size classes in the generated length data.
Estimated Parameters		
SL_{50}	50	Length at which 50% of the population is selected by the fishery.
SL_{95}	55	Length at which 95% of the population is selected by the fishery.
F/M	-	Ratio of fishing mortality (F) to the natural mortality rate. Set at various levels in the simulations.
SPR	-	The spawning potential ratio. Calculated from the input biological parameters and the estimated exploitation parameters.

Table 2 The estimated F/M, selectivity parameters, and the resulting estimate of the spawning potential ratio from the LB-SPR and the GTG LB-SPR estimation models for the four reef fish species from Palau. The input parameters were fixed at the most likely values identified for these species by Prince et al. (2015a).

| Species		SPR	F/M	S_{L50} (mm)	S_{L95} (mm)	M/K	L_∞ (mm)	CVL_∞	L_{50} (mm)	L_{95} (mm)
				Estimated Parameters			**Input Parameters**			
H. longiceps	LB-SPR	0.05	6.6	277	315	1.07	423	0.1	300	330
	GTG LB-SPR	0.11	4.3	271	312					
L. gibbus	LB-SPR	0.08	4.4	221	251	0.41	343	0.1	257	320
	GTG LB-SPR	0.12	3.4	218	248					
L. rubrioperculatus	LB-SPR	0.26	2.5	232	268	0.62	306	0.1	214	270
	GTG LB-SPR	0.39	1.7	229	267					
V. louti	LB-SPR	0.04	4.1	208	274	0.86	483	0.1	285	350
	GTG LB-SPR	0.06	3.5	201	266					
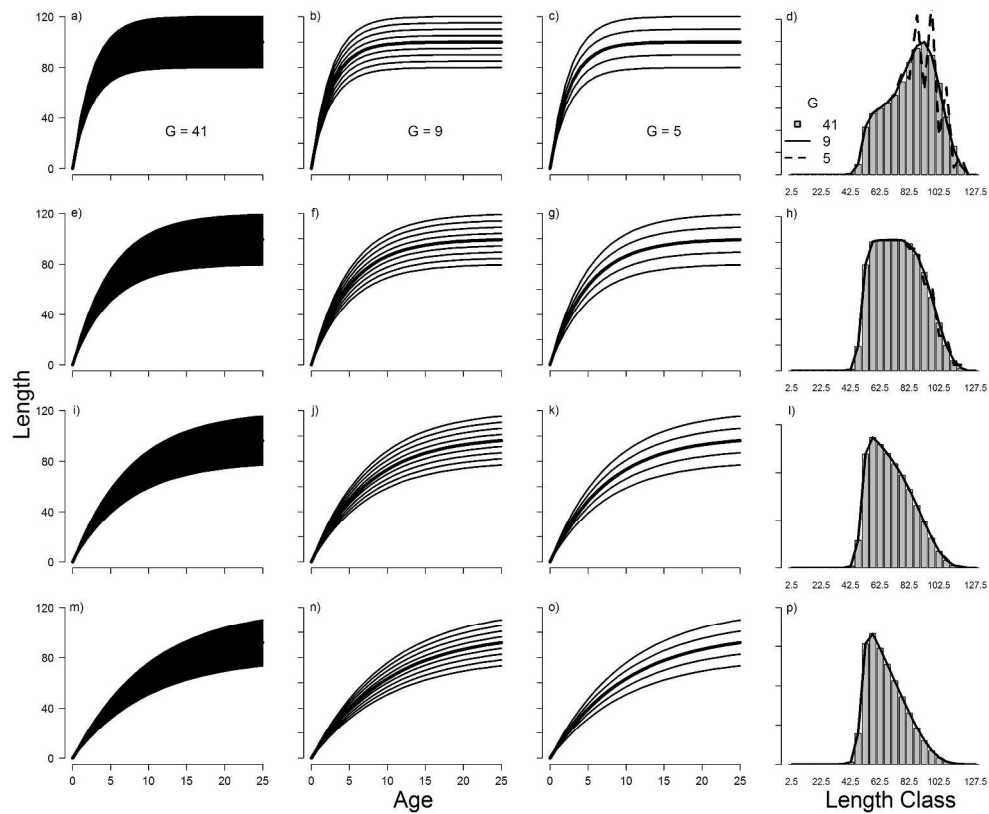
Figure 1. The individual von Bertalanffy growth curves of simulations with 41, 9 and 5 growth-type-groups (G; columns 1, 2 and 3 respectively) and the resulting expected size composition (column 4) with grey bars representing the size structure generated with G=41, solid black line when G=9, and dashed black line when G=5. Panels a-d show the simulations when $M/K = 0.5$, e-h $M/K = 1.0$, i-l $M/K = 1.5$, and m-p $M/K = 2.0$. Due to the small interval between the growth-type-groups, it is not possible to distinguish the 41 individual growth curves in column 1. The thick line in columns 2 and 3 represent the central growth-type-group which shares the L_∞ parameter with the population as a whole.
299x249mm (300 x 300 DPI)
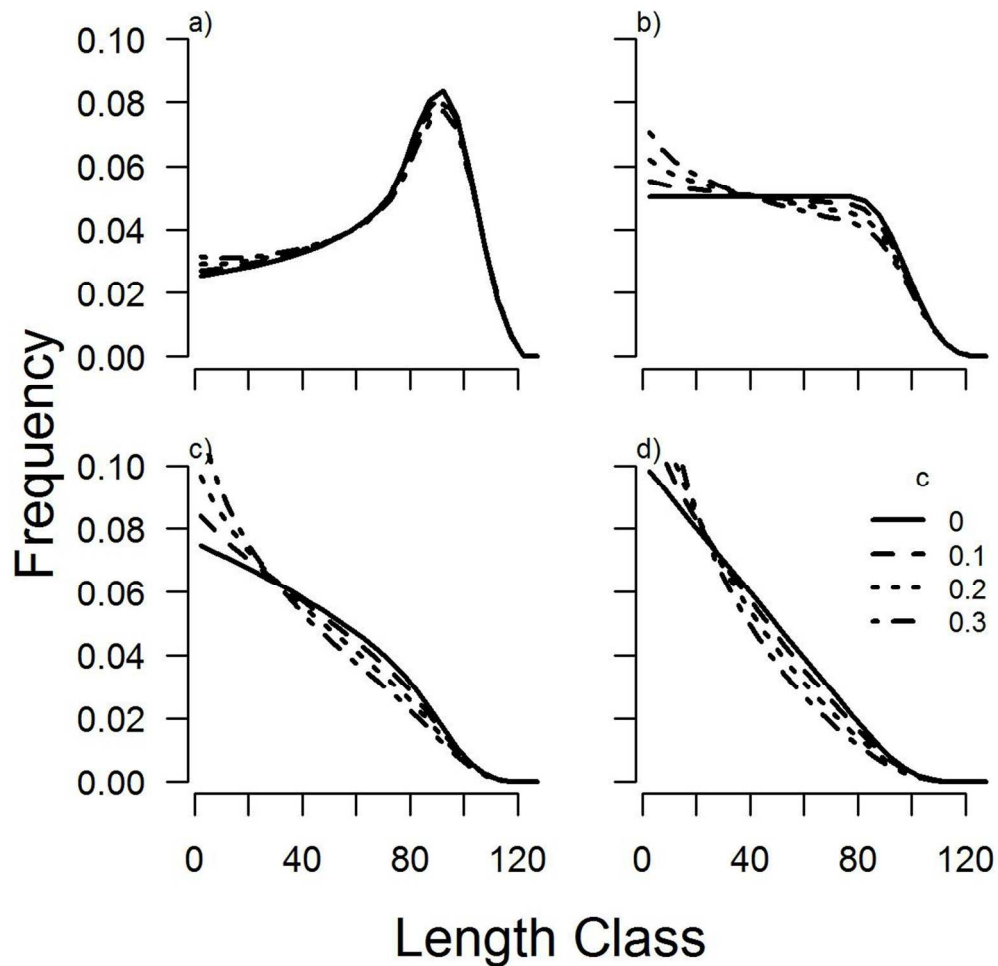
Figure 2. Simulations from the GTG LB-SPR model showing the expected equilibrium \r\nunfished length composition for four different values of M/K (0.5, 1.0, 1.5, and 2.0 for a, b, c, and d respectively) and increasing values of c, the parameter controlling size-dependent natural mortality.
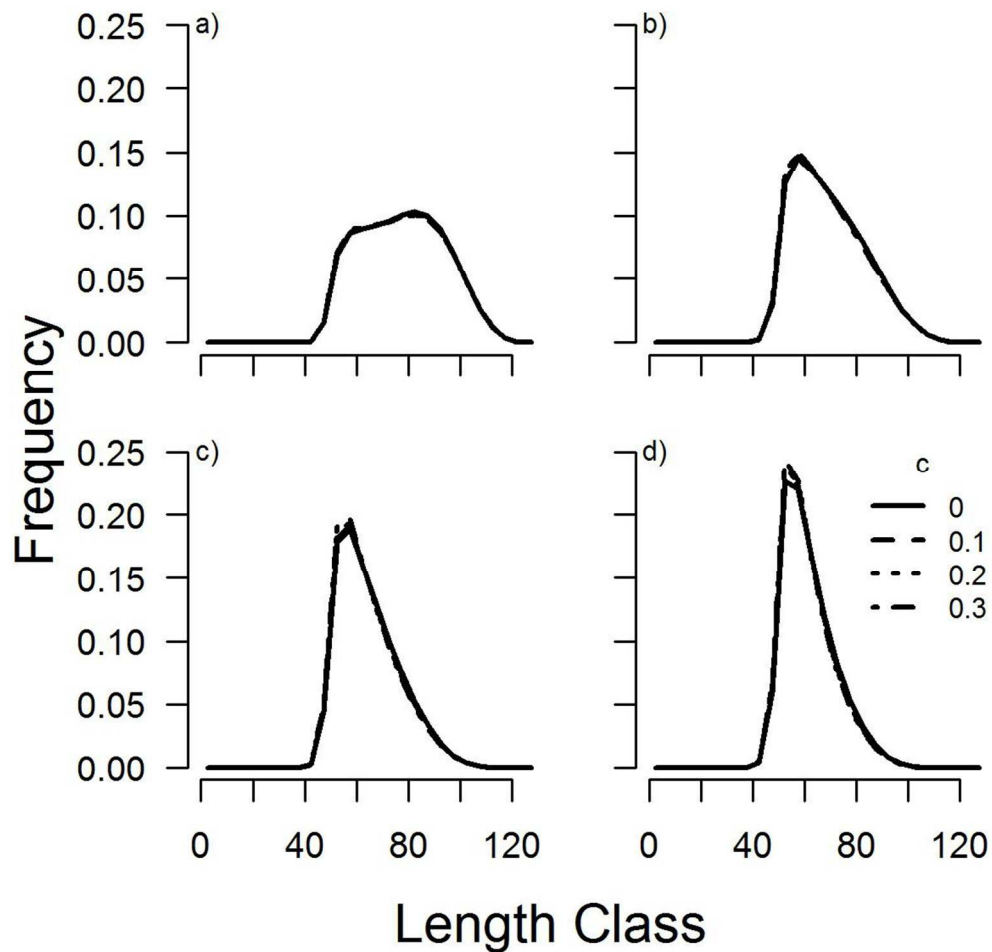99x99mm (300 x 300 DPI)

Figure 3. The expected equilibrium size composition of the catch for a) $M/K = 0.5$, b) 1.0, c) 1.5 and d) 2.0, at SPR=0.50, with four different values of size-dependent natural mortality coefficient (solid, dashed, dotted, and dash-dotted lines for c=0, 0.1, 0.2, and 0.3 respectively). The differences between the four size-dependant natural mortality rates are almost indistinguishable on the plot. The other life history parameters are shown in Table 1.
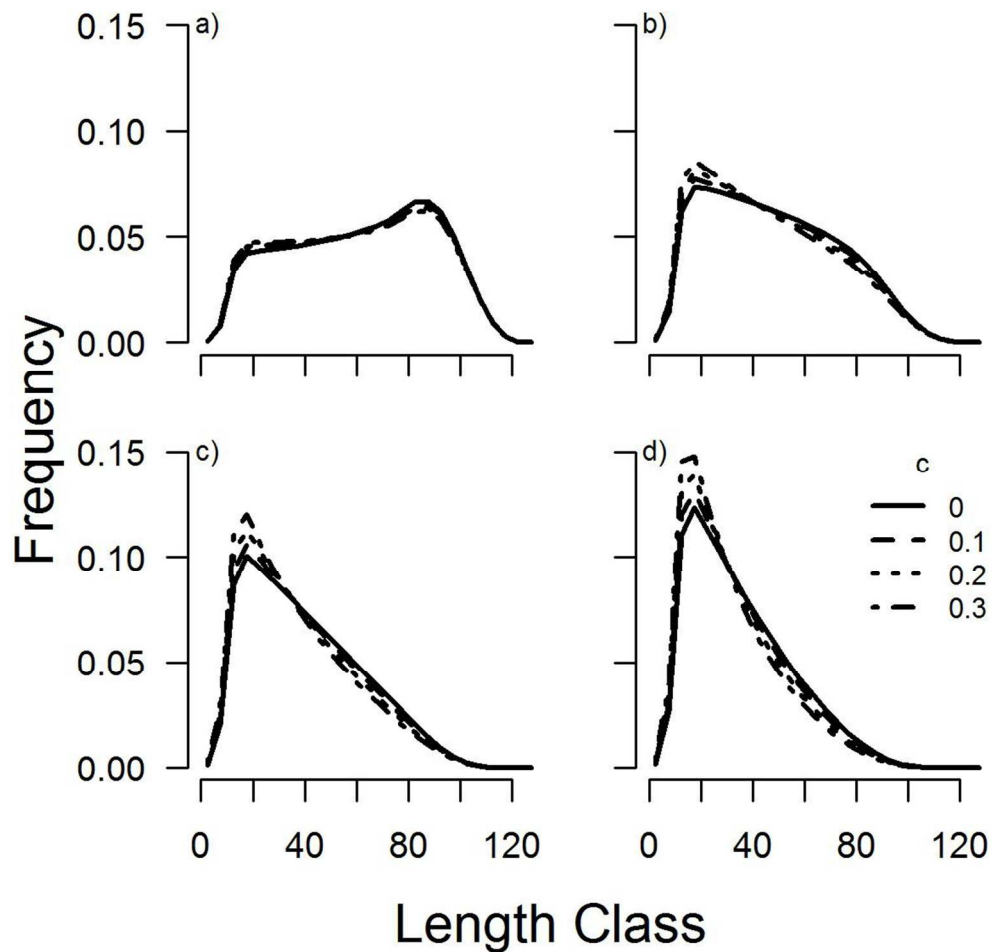99x99mm (300 x 300 DPI)

Figure 4. The expected equilibrium size composition of the catch for a) $M/K = 0.5$, b) 1.0, c) 1.5 and d) 2.0, at SPR=0.50, and with a smaller size at selectivity (S_{L50} and S_{L95} set to 10 and 15 respectively, and with four different values of size-dependent natural mortality coefficient (solid, dashed, dotted, and dash-dotted lines for $c = 0$, 0.1, 0.2, and 0.3 respectively). The differences between the four size-dependant natural mortality rates are more clearly visible in these simulations. The other life history parameters are shown in Table 1. 99x99mm (300 x 300 DPI)
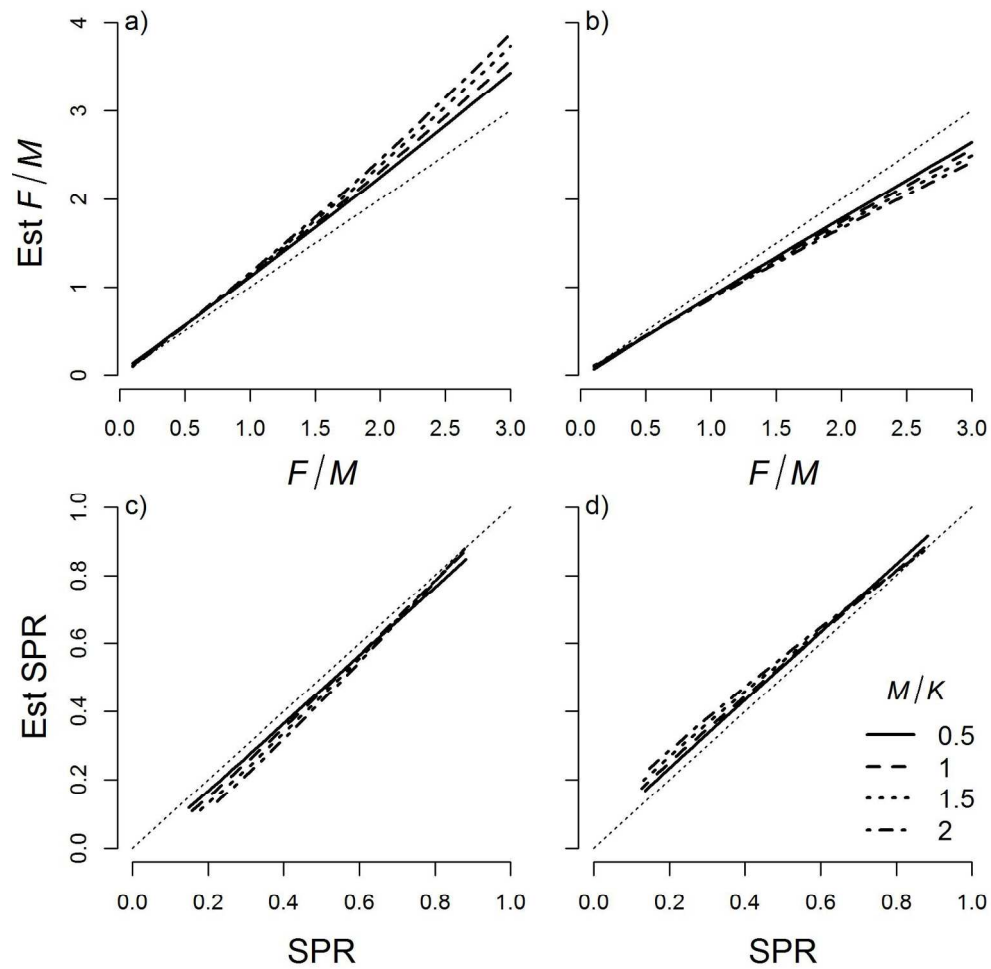
Figure 5. The simulated (x-axis) and estimated (y-axis) values of *F/M* and SPR when the size data was generated with the GTG LB-SPR model and the parameters estimated with the LB-SPR model (panels a and c) and vice versa (panels b and d), for four ratios of *M/K* (*M/K* = 0.5, 1.0, 1.5 and 2.0 for the solid, dashed, dotted, and dash-dotted lines respectively.
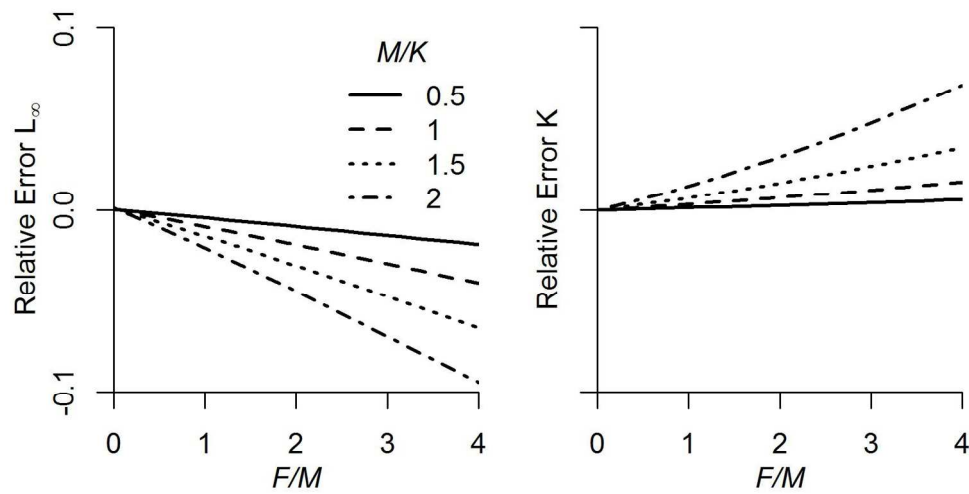159x159mm (300 x 300 DPI)

Figure 6. The relative error in the estimated L∞ and *K* parameters when the von Bertalanffy growth equation is fitted to length-at-age data from a population under increasing levels of exploitation. Lee's Phenomenon results in the selective removal of faster growing individuals from the population, which depresses the observed mean length-at-age and results in biased estimates of the growth parameters, especially for the highest *M/K* species under high fishing mortality. Four different life history types were examined: *M/K* = 0.5, 1.0, 1.5, and 2.0 (solid, dashed, dotted, and dash-dotted lines respectively). See Table 1 for other biological parameters.
149x74mm (300 x 300 DPI)